Enantiodiscrimination in NMR spectra and X-ray structures of diastereomeric salts of *trans*-4-(4-fluorophenyl)-3-hydroxymethyl-1-methylpiperidine with (*S*)-Mosher acid

Hana Navrátilová,*[a] René de Gelder[b] and Zdeněk Kříž[c]

[a] *Department of Organic Chemistry, Faculty of Science, Masaryk University, Kotlářská 2, 611 37 Brno, Czech Republic. E-mail: hanavra@chemi.muni.cz; Fax: 420 5 411 29 641; Tel: 420 5 411 29 311*

[b] *Crystallography Laboratory, Department of Inorganic Chemistry, Faculty of Science, University of Nijmegen, Toernooiveld 1, 6525 ED, Nijmegen, The Netherlands. E-mail: rdg@sci.kun.nl*

[c] *National Centre for Biomolecular Research, Faculty of Science, Masaryk University, Kotlářská 2, 611 37 Brno, Czech Republic. E-mail: zdenek@ncbr.chemi.muni.cz*

Received (in Cambridge, UK) 23rd July 2002, Accepted 8th October 2002
First published as an Advance Article on the web 28th October 2002

Signal anisochrony ($\Delta\delta$) in NMR spectra of racemic *trans*-4-(4-fluorophenyl)-3-hydroxymethyl-1-methylpiperidine **1** induced on the formation of diastereomeric salt complexes with (*S*)-Mosher acid **2** showed a strong dependence on solvent polarity, concentration, stoichiometric ratio and enantiomeric composition. X-Ray structures of the salts, **3a** and **b**, revealed that the conformations of the protonated base in ion pairs are very similar with respect to interatomic distances, bond and torsion angles but the mutual orientation of counterions in ion pairs differs significantly. It is suggested that the conformations of transient diastereomeric complexes in solution, responsible for $\Delta\delta$, resemble those in the solid state. Furthermore, *ab initio* calculations performed on the optimized X-ray geometries of both ion pairs showed that the free energy of **3a** is lower than that of **3b**. This implies that the association constant for the formation of **3a** is higher than that of **3b**.

Introduction

A prerequisite in determining the enantiomeric purity of a chiral compound by NMR spectroscopy is to induce anisochrony ($\Delta\delta$) in NMR spectra of enantiomers using a chiral auxiliary.[1] This methodology, based on external diastereotopicity, was first proposed by Raban and Mislow[2] and subsequently elaborated by Pirkle[3] who employed non-racemic chiral solvents to differentiate NMR signals of enantiomers. The formation of ionic non-covalent diastereomers between an enantiopure base and a racemic acid, first reported by Horeau and Guetté,[4] has been applied to the enantiomeric analysis of a variety of chiral acids in the presence of enantiopure amines[5,6] and *vice versa*.[7,8] Depending on the degree of chiral recognition occurring between the base and the acid, the resulting short-lived diastereomeric salt complexes in solution may adopt distinct conformations that give rise to the anisochrony of enantiomer NMR signals. Despite a number of applications of the approach developed by Horeau and Guetté, relatively little is known about the specific chirality-dependent interactions in the particular diastereomeric salt complexes which are responsible for the appearance of $\Delta\delta$.

Enantiopure Mosher acids are well established chiral derivatizing reagents currently employed in determining the enantiomeric composition[9] and absolute configuration[10] of chiral amines or alcohols by means of NMR spectroscopy of the resultant diastereomeric esters and amides. Furthermore, due to the enhanced acidity and the presence of polarized substituents (trifluoromethyl, methoxy) and the anisotropic phenyl group, Mosher acids are also efficient chiral solvating agents,[8] inducing large non-equivalence in NMR spectra of chiral amines. Moreover, enantiopure Mosher acids have recently been used as chiral ligands in rhodium complexes[11] for chiral recognition of various chiral compounds by means of NMR spectroscopy.

In the present paper we attempt to explain the mechanism by which the (*S*)-Mosher acid **2** exercises its influence on the NMR spectral behaviour of enantiomeric *trans*-4-(4-fluorophenyl)-3-hydroxymethyl-1-methylpiperidines **1a** and **1b** (Fig. 1). Enantiomer **1a** with the (3*S*,4*R*)-configuration[12] is an important intermediate in the industrial synthesis of the antidepressive drug paroxetine **4**[13] The enantiomeric analysis of **1a** by means of NMR spectroscopy in the presence of (*S*)-Mosher acid **2** has been reported recently.[14]

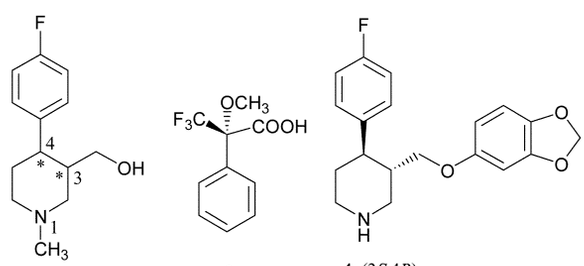

1a: (3*S*,4*R*)
1b: (3*R*,4*S*)

2

4: (3*S*,4*R*)

Fig. 1 Structures of compounds.

Results and discussion

NMR spectroscopy of diastereomeric salts

As illustrated in Scheme 1, a neutralization reaction between (*S*)-Mosher acid **2** and racemic **1** produces two diastereomeric

Table 1 ^{1}H, ^{13}C and ^{19}F NMR chemical shifts of selected nuclei in **3a** and **3b** (measured for a mixture containing 60% of **3a** and 40% of **3b**, 113 mM) and in free **1** (105 mM) in benzene-d_6 and chloroform-d

	In benzene[a]				In chloroform[a]			
Nucleus	δ (**3a**)	δ (**3b**)	$\Delta\delta$[b]	δ (**1**)	δ (**3a**)	δ (**3b**)	$\Delta\delta$[b]	δ (**1**)
H-2e	3.580	3.660	−0.080	3.189	3.658	3.742	−0.084	3.149
H-5e	1.184	1.089	0.095	1.513	1.863	1.815	0.048	1.777
H-6e	2.575	2.435	0.140	2.666	3.607	3.466	0.141	2.909
H-7 (NCH_3)	2.034	2.039	−0.005	2.132	2.719	2.719	0	2.302
H-8d[c]	3.012	3.089	−0.077	3.007	3.102	3.141	−0.039	3.191
H-8u[c]	3.249	3.348	−0.099	3.206	3.301	3.361	−0.060	3.372
H-10,14	6.925	6.829	0.096	6.885	7.015	7.015	0	7.135
C-2[d]	57.575	57.522	0.053	60.017	57.038	57.038	0	59.403
C-3[d]	42.409	42.231	0.178	44.663	41.239	41.239	0	44.188
C-4[d]	41.624	41.749	−0.125	43.989	41.010	41.111	−0.101	43.623
C-5[d]	31.365	31.365	0	34.685	30.837	30.887	−0.050	34.338
C-7 (NCH_3)[d]	43.337	43.266	0.071	46.553	43.504	43.504	0	46.419
C-8[d]	62.000	62.089	−0.089	63.519	61.391	61.450	−0.059	63.468
F-1	−115.653	−115.764	0.111	−116.920	−115.140	−115.171	0.031	–[e]

[a] Digital resolution: 0.22 Hz/point in ^{1}H NMR spectra, 1.38 and 0.91 Hz/point in ^{13}C NMR spectra recorded at 75.47 and 100.62 MHz, respectively, 0.27 Hz/point in ^{19}F NMR spectra. [b] $\Delta\delta$ was calculated as follows: $\Delta\delta = \delta$(**3a**) − δ(**3b**), δ(**3a**) and δ(**3b**) are chemical shifts of a particular nucleus in **3a** and **3b**, respectively. [c] Protons H-8d (downfield) and H-8u (upfield) are diastereotopic protons at C-8. [d] Carbon chemical shifts of **3a** and **3b** were measured at 282 K at 100.62 MHz; those of free racemic **1** at 303 K at 75.47 MHz. [e] A fluorine spectrum of this sample was not recorded.

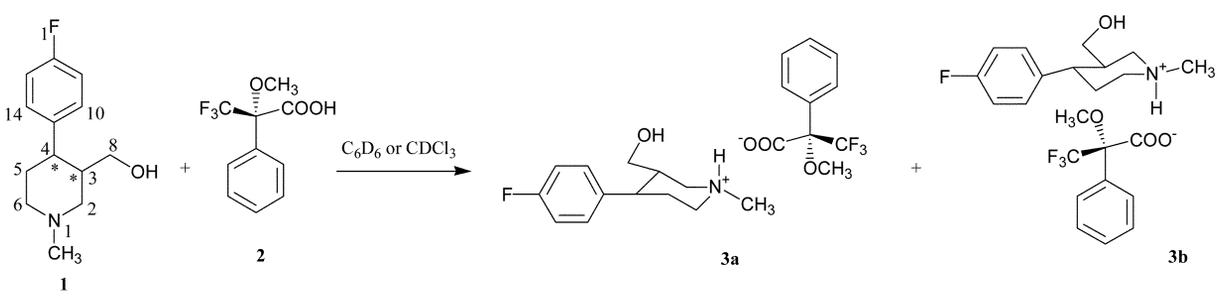

Scheme 1 Diastereomeric salt complexes, **3a** and **b**, formed between *rac*-**1** and (*S*)-Mosher acid **2**.

salts: (3*S*,4*R*)-piperidinium (*S*)-Mosher carboxylate **3a** and (3*R*,4*S*)-piperidinium (*S*)-Mosher carboxylate **3b**. NMR spectra of the salts show significant differences in the region of resonances due to the piperidinium cation. This spectral anisochrony $\Delta\delta$, expressed as the difference between the chemical shift of the particular nucleus in **3a** and that in **3b**, arises from two causes[1] that might be mutually dependent. Firstly, the protonated enantiomeric bases have different magnetic surroundings resulting from distinct transient conformations of the particular diastereomeric salt in solution.[15,16] Secondly, association constants for the formation of the two diastereomeric complexes may not be equal.[17,18]

Table 1 provides an overview of proton, carbon and fluorine chemical shifts measured for free *rac*-**1** and for a mixture consisting of 60% of **3a** and 40% of **3b** in deuterated benzene and chloroform. Signals of the salts were broadened as a consequence of fast chemical exchange between free and bonded counterions in solution. The spectral non-equivalence $\Delta\delta$ was detected for nuclei of the piperidinium moiety which are located in close proximity to the complexation site at N-1 and to the chiral centre at C-3 and C-4. It is obvious that the surrounding medium has a profound effect on the magnitude of $\Delta\delta$. In the benzene solution of the mixture of salts more nuclei became anisochronous and the resultant non-equivalence $\Delta\delta$ was larger compared with that in the chloroform solution. This can be attributed to an additional shielding effect of benzene. In diastereomeric salts the interaction between counterions is very strong and is determined primarily by hydrogen bonding. Therefore, in non-polar solvents the counterions are preferably associated in neutral complexes solvated by solvent molecules, while in polar solvents a weak hydrogen bonding between ions and solvent contributes to the diminishing or even disappearance of $\Delta\delta$.[1] As a result of the protonation of the piperidine nitrogen in **1** the chemical shifts of most signals significantly changed compared with those in free base. Thus, H-2e, 6e, 5e and 7 (N-methyl group) in **3a** and **b** in chloroform, and F-1 in benzene exhibited a considerable downfield shift while the upfield shift was observed for carbons C-2,3,4,5 and 8 in both solvents. However, in both solvents the $\Delta\delta$s were of the similar values. Furthermore, the magnitude and sense of spectral non-equivalence $\Delta\delta$ for the particular nuclei reflect the presence of different magnetic surroundings indicating the existence of specific conformations of salt complexes in solution.[15] In comparison with **3b** the protons H-2e, 7, 8u, 8d and carbons C-4, 8 in **3a** are more magnetically shielded whereas nuclei H-5e, 6e, 10, 14 and C-2, 3, 7 and F-1 in **3a** were relatively deshielded. The relative magnetic shielding suggests that the respective nuclei in the distinct solution conformations of the complexes are situated in the shielding region of the phenyl ring of (*S*)-Mosher carboxylate. This may account for the upfield shift of H-2e, H-5e and 7 in **3a** implying their close proximity to the phenyl group of the anion. Similarly, the shielding of *ortho* protons and fluorine in the 4-fluorophenyl substituent in **3b** may also result from the anisotropic effect of the phenyl ring in the (*S*)-Mosher carboxylate being proximate to them. Furthermore, protons H-2e and H-6e exhibit quite large non-equivalence showing almost no change with solvent. Moreover, in **3a** the proton H-2e resonates at a lower frequency to that in **3b** while the signal due to H-6e is shifted downfield from that in **3b**. This is likely to be caused by the differential proximity of these protons to the magnetically anisotropic carboxylate carbonyl group, indicating that H-6e in **3a** and H-2e in **3b** are located in the deshielding region of the carbonyl π-system.[19] This finding has been corroborated by the X-ray structural studies of the ion pairs (Fig. 6), which are discussed further in the text.

Table 2 Dependence of $\Delta\delta_F$ on the concentration of salt of *rac*-**1** with **2**, recorded in C_6D_6 at 297 K

Concentration/mM	$\Delta\delta_F$ (ppm)[a]
139.6	0.059
100.0	0.065
78.2	0.066
61.2	0.068
48.9	0.070
24.5	0.072
12.2	0.069
6.1	0.066
1.5	0.050

[a] $\Delta\delta_F = \delta_F$(**3a**)–$\delta_F$(**3b**), δ_F(**3a**) and δ_F(**3b**) are fluorine chemical shifts in **3a** and **3b**; digital resolution was 0.21 Hz per point.

^{1}H-^{1}H NOESY and ^{1}H-^{19}F HOESY experiments were carried out on both salts in order to detect intermolecular contacts between the counterions. The existence of such contacts would indicate a high degree of association of counterions in ion pairs and could help to predict the conformations of diastereomeric complexes in solution, as reported previously by Pirkle.[16] However, the results of both experiments were rather too ambiguous to provide consistent evidence about the close spatial proximity of the counterions.

Once non-equivalence is detected for some nuclei in the diastereomeric complexes, its magnitude can be optimized.[6] Of all resolved nuclei, the fluorine in the 4-fluorophenyl group of **1** was found to be the most sensitive probe to monitor variations of $\Delta\delta_F$ with different experimental parameters such as concentration, stoichiometry and enantiomeric composition. Under the given experimental conditions the fluorine spectrum consists of three resonances. Two of them can be detected at *ca*. −115 ppm and belong to the fluorines of the 4-fluorophenyl group in **3a** (downfield resonance) and **3b** (upfield resonance); the third fluorine signal, due to the CF_3 group in (*S*)-Mosher carboxylate, was at *ca*. −70 ppm, as referenced to $CFCl_3$.

Table 2 shows the variation of $\Delta\delta_F$ with the salt concentration in benzene. $\Delta\delta_F$ was somewhat insensitive to an increasing concentration of salts, remaining quite large over a wide concentration interval from *ca*. 6 to 100 mM and reaching a maximum value of 0.072 ppm for 24.5 mM solution. However, at high concentrations (>100 mM) its magnitude decreased, probably due to the formation of ion aggregates in solution,[8] while at very low concentrations (<6 mM) it diminished due to the increasing dissociation of ion pairs.

The effect of stoichiometry on $\Delta\delta_F$ is illustrated in Fig. 2. A sharp increase of $\Delta\delta_F$ was noted for *rac*-**1** in benzene at the acid:base ratio ranging from 0.5–1. The $\Delta\delta_F$ reached its maximum value of 0.065 ppm at the ratio of *ca*. 1. This can be attributed to the formation of the salt. But at higher stoichiometric ratios the $\Delta\delta_F$ drops considerably, reaching its minimum

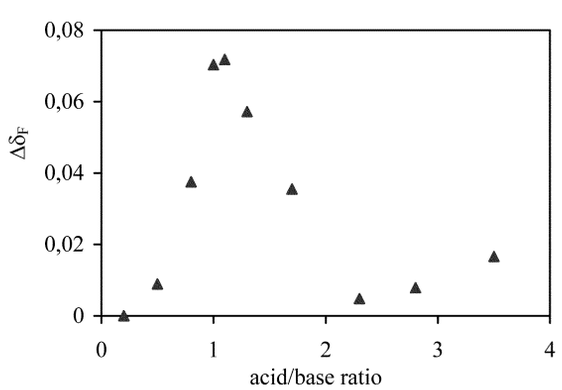

Fig. 2 Variation of $\Delta\delta_F$ with a **2**:*rac*-**1** ratio, recorded for 30 mM solutions of *rac*-**1** in C_6D_6 at 297 K.

at a ratio of *ca*. 2, followed by a mild increase to *ca*. 0.015 ppm at a ratio of 3.5. A similar dependence was also observed for equatorial protons H-2, 5 and 6 of the piperidine. By contrast, the $\Delta\delta_H$ for the diastereotopic protons H-8d and H-8u at the equimolar acid:base ratio was 0.066 and 0.041 ppm, respectively, and increased to a limiting value of 0.069 ppm for H-8u and 0.057 ppm for H-8d when the acid:base ratio increased from 2 to 3.5 (Fig. 3). A singlet due to the N-methyl protons of

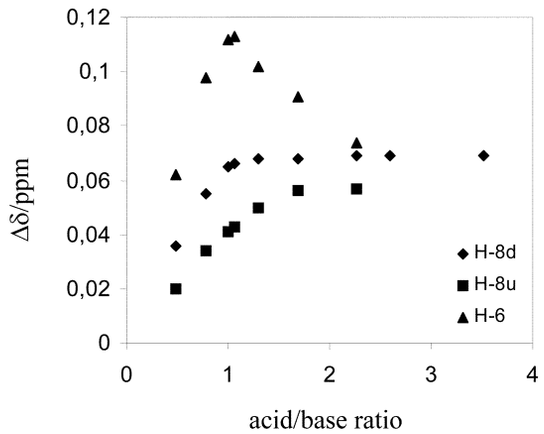

Fig. 3 Variation of $\Delta\delta_H$ for diastereotopic protons H-8d and H-8u and for H-6e in *rac*-**1** (30 mM) with stoichiometric ratio, recorded in C_6D_6 at 297 K.

the piperidinium showed splitting only for the acid:base ratios below and above 1. This interesting spectral behaviour might result from the displacement of dissociation equilibrium[6,8] caused by acid dimerization favoured in a non-polar solvent. The variation of the $\Delta\delta$s for the fluorine and some protons attached to the piperidine ring implies that at a stoichiometric ratio of *ca*. 1, when the maximum $\Delta\delta$ is observed, the salt complexes adopt their distinct conformations. However, the $\Delta\delta_H$ for exocyclic diastereotopic protons at C-8 appears to be affected only by the protonation of nitrogen.

The effect of the enantiomeric composition on the magnitude of $\Delta\delta_F$ was examined in benzene and chloroform solutions at 30 mM salt concentration. In chloroform solutions the shift difference increased from 0 ppm (−60%ee **3a**) to 0.048 ppm (89%ee **3a**). For racemic substrate **1** the value of $\Delta\delta_F$ was 0.025 ppm. At the ee. values below −80%, the fluorine resonances become isochronous. In benzene, $\Delta\delta_F$ for **3a** with enantiomeric composition ranging from −70 to +70% ee was nearly linear. It is particularly interesting to observe that the chemical shift of **3a** remained almost unaffected with the increasing enantiomeric purity of **3a**, while the fluorine resonance in **3b** moved significantly upfield with the decreasing amount of **3b** in the sample (Fig. 4). Outside this range the dependence becomes non-linear as the $\Delta\delta$ function is probably governed by dissociation. A similar behaviour was reported for analogous diastereomeric complexes and is probably a consequence of the non-equivalence of association constants.[6,17] For the diastereotopic protons H-8d and H-8u the $\Delta\delta$ gradually decreased with a decreasing content of **3a** in a mixture and changed its sense when the enantiomeric composition of **1a** was as low as −38% ee.

The NMR spectral behaviour of the transient diastereomeric salt complexes indicates the existence of specific conformations of the salts in solution and it also suggests that the energies and association constants for their formation are considerably different.

X-Ray structures of diastereomeric salts

The crystal structures of the diastereomeric salts, **3a** and **b**, (Fig. 5) are featured by an infinite one-dimensional hydrogen-

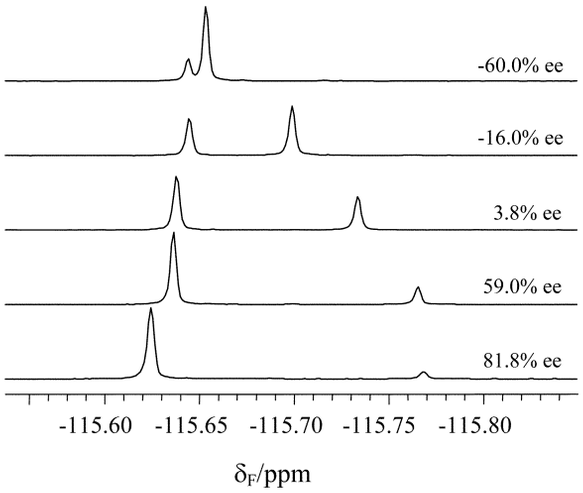

Fig. 4 Variation of fluorine chemical shift of **3a** (downfield signal) and **3b** (upfield signal) with enantiomeric excess of **3a** in the presence of **2** (1.05 equiv.), recorded for 30 mM solutions in C_6D_6 at 297 K.

bond chain parallel to the *b*-axis, linking the piperidinium cations and (*S*)-Mosher carboxylates. The aryl groups of the counterions are pointing away from the hydrogen-bond chain forming hydrophobic columns in which the π-π interactions between the 4-fluorophenyl group of a cation and the phenyl ring of an anion can be recognized.

The crystallographic data and structure refinement for diastereomeric salts **3a** and **b** are provided in Table 3. Both crystals are monoclinic and belong to the $P2_1$ space group. Crystal density of **3a** is slightly higher than that of **3b** which indicates that the crystal packing of **3a** is more efficient. This fact may also account for different melting points of the crystals;[18] the melting point of **3a** was 133–134 °C, whereas **3b** melted at 117–119 °C.

The presence of two types of intermolecular hydrogen bonds is a significant feature detected in both crystal structures. The diastereomeric complex formed between (*S*)-Mosher acid **2** and an enantiomeric base **1a** or **1b** has two hydrogen-bond donors (OH groups in hydroxymethyl and carboxy) and two acceptors (N and CO). One hydrogen bond is formed between the nitrogen of the piperidininium moiety and the oxygen of the (*S*)-Mosher carboxylate, the other connects the hydroxymethyl group of the piperidinium moiety and the carboxylic oxygen of the (*S*)-Mosher carboxylate. As seen in Table 4, the lengths of the hydrogen bonds in both ion pairs and the corresponding angles in **3a** fall in the interval expected for analogous hydrogen bonds.[20] However, the angle of N(1) ··· H(1B) ··· O(3) in **3b** is the least linear of the hydrogen bonds. This is thought to result from the mutual configuration of counterions which tends to minimize repulsive interactions between the aromatic rings.

It is obvious that the hydrogen bonding affects not only the conformations of the piperidinium cation and the (*S*)-Mosher carboxylate but it is also a key factor in controlling the mutual orientation of the counterions in ion pairs. As seen in Fig. 6, the piperidinium ring in **3a** and **3b** adopts the chair conformation with all three substituents (the 4-fluorophenyl at C4, the hydroxymethyl at C3 and N-methyl) in equatorial positions. Furthermore, the conformations of both protonated enantiomeric bases are essentially identical with respect to interatomic distances, bond and torsional angles. In contrast, the conformation of the (*S*)-Mosher carboxylate in **3a** differs considerably from that in **3b**, as demonstrated by the torsional angles of the acid moieties in both ion pairs (Table 5). Similar findings were reported for analogous diastereomeric salts prepared in optical resolutions.[21] Thus, in **3a** the methyl in the methoxy group of the (*S*)-Mosher carboxylate points towards the aromatic ring and the bond C(16)–C(17) lies almost in the plane of the aromatic ring whereas in ion pair **3b**, the methyl in the methoxy group is oriented away from the plane of the phenyl ring and the trifluoromethyl group is nearly perpendicular to the plane of the phenyl ring. For the (*S*)-Mosher carboxylate in both **3a** and **3b**, O2 points to the trifluoromethyl group and O3 to the methoxy group. This is a consequence of attractive and repulsive forces in an ion pair which also lead to the specific mutual orientation of counterions. The differences between the structures of ion pairs, **3a** and **3b**, are striking. The T-arrangement of the aromatic rings of counterions in **3b** suggests the existence of a CH ··· π hydrogen-bonding interaction[22] of protons H-13 and H-14 of the fluorophenyl group with the π-cloud of the phenyl ring in the anion; the H(13)–C(22) and H(14)–C(23) interatomic distances are 2.90 and 2.96 Å, respectively. In the ion pair **3a**, this interaction is absent because both aromatic groups are distant from one another. In a benzene solution of **3b**, however, this interaction may be overwhelmed by stacking with the bulky aromatic solvent.

The formation of the intermolecular hydrogen bond between the positively charged nitrogen N(1) of the piperidinium cation and the carboxylic oxygen of the (*S*)-Mosher carboxylate is clearly the driving force for ion pairing in solution where it is thought to control the geometries and stabilities of the ion pairs.

Free energy computations

According to the results of the NMR studies, the association constants for the formation of salt complexes **3a** and **b** in solution may not be equal. To prove this we decided to compute the free energies of both ion pairs in order to find out which of the two diastereomeric complexes is more stable and therefore might have a higher association constant.[23,24]

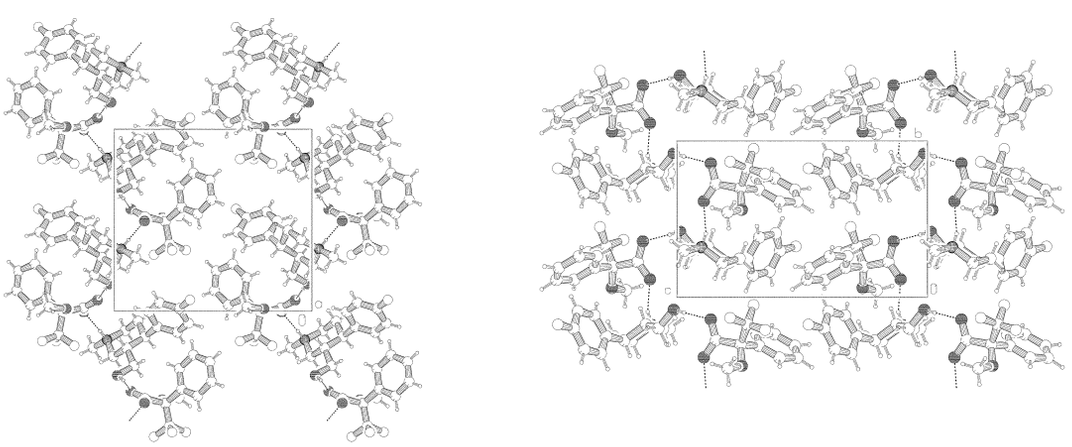

Fig. 5 Crystal structures of **3a** (left) and **3b** (right); crystal packing as seen along the *a*-axis (drawn in Pluton).[30]

Table 3 Crystallographic data and structure refinement for diastereomeric salts **3a** and **3b**

Parameters	**3a**	**3b**
Empirical formula	$C_{23}H_{27}F_4N_1O_4$	$C_{23}H_{27}F_4N_1O_4$
Molecular weight/g mol^{-1}	457.46	457.46
T/K	293(2)	293(2)
Crystal system	monoclinic	monoclinic
Space group	$P2_1$	$P2_1$
Crystal size/mm^3	0.54 × 0.38 × 0.05	0.45 × 0.39 × 0.14
a/Å	7.3090(2)	8.9615(2)
b/Å	12.0081(4)	8.97716(19)
c/Å	13.0629(3)	14.7286(7)
β/°	90.441(2)	101.862(5)
V/Å^3	1146.46(5)	1159.59(7)
Z	2	2
D_c/mg m^{-3}	1.325	1.310
θ-range for data collection/°	3.38–70.01	3.07–69.86
Absorption coefficient/mm^{-1}	0.954	0.943
Reflections collected/independent	2378/2279	2411/2273
R_{int}	0.0235	0.0141
Final R indices [$I > 2\sigma(I)$]	$R_1 = 0.0468$, w$R_2 = 0.1535$	$R_1 = 0.0337$, w$R_2 = 0.0911$
R indices (all data)	$R_1 = 0.0495$, w$R_2 = 0.1573$	$R_1 = 0.0359$, w$R_2 = 0.0936$
Largest diff. peak and hole/e Å^{-3}	0.181 and −0.220	0.164 and −0.146
No. data/restraints/parameters	2279/1/300	2273/1/398

Table 4 Parameters of hydrogen bonds in salts **3a** and **3b**

D–H ··· A	D ··· H/Å	H ··· A/Å	D ··· A/Å	Angle/°
In **3a**				
N(1)–H(1B) ··· O(2)	0.8936	1.7790	2.6596	168.01
O(1)–H(1A) ··· O(3)	0.8589	1.8754	2.7222	168.37
In **3b**				
N(1)–H(1B) ··· O(3)	0.8126	1.8831	2.6462	155.99
O(1)–H(1A) ··· O(2)	0.7559	1.9345	2.6903	178.97

Table 5 Selected torsional angles for (*S*)-Mosher carboxylate in diastereomeric ion pairs **3a** and **3b** (with standard deviations in parentheses)

Torsional angle	**3a**	**3b**
C(19)–C(16)–O(4)–C(18)	47.62(47)	173.93(24)
C(15)–C(16)–O(4)–C(18)	165.26(36)	−64.95(29)
O(4)–C(16)–C(19)–C(20)	−129.87(44)	−34.02(31)
C(17)–C(16)–C(19)–C(20)	−6.61(55)	83.69(30)
C(15)–C(16)–C(19)–C(20)	112.98(44)	−155.88(25)
C(19)–C(16)–C(15)–O(2)	−65.83(39)	−84.99(28)
C(19)–C(16)–C(15)–O(3)	113.90(38)	93.85(26)
C(17)–C(16)–C(15)–O(2)	58.20(38)	33.81(32)
C(17)–C(16)–C(15)–O(3)	−122.06(39)	−147.36(23)

Conformations of diastereomeric ion pairs were analysed using a quantum mechanics approach. Geometry optimization started with the X-ray structures of ion pairs **3a** and **b**. The complexes were kept neutral; the angle and length of the hydrogen bond as listed in Table 4 were used as constraints during the initial optimization. The resultant 'partially' optimized structures of the ion pairs were allowed to fully relax in order to find the geometry optimum. This was followed by a single-point energy calculation using the GAUSSIAN program package.[25] All optimizations were performed *in vacuo* using the HF method with 6-31G(d,p) basis set, which includes polarization functions at the hydrogen atoms, enabling a reliable description of hydrogen bonds, and which has been found to provide sound results for similar systems.[26]

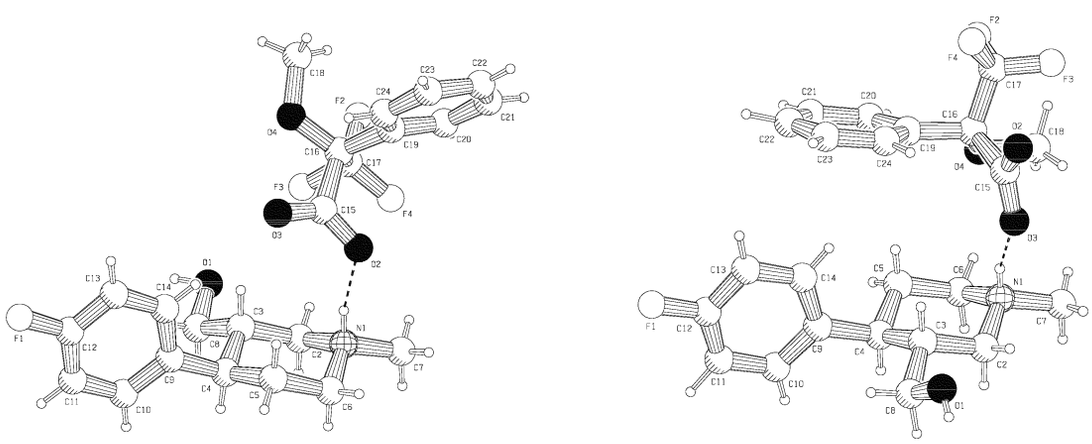

3a **3b**

Fig. 6 The X-ray structures of ion pairs **3a** and **3b**

Table 6 Differences between the optimized and X-ray structures, expressed as root-mean-square deviations for each ion pair (RMSD)

	RMSD for **3a**	RMSD for **3b**
Full-X-ray	0.83	0.25
Partial-X ray	0.54	0.96
Partial-full	0.53	0.79

A comparison of optimized conformations with X-ray structures expressed in RMSDs for the superimposition of structures is provided in Table 6. The differences between X-ray structures and optimized conformations can be explained in terms of crystal packing effects being operative in the solid state but not included in these calculations, which were performed on the structures in the gaseous phase. However, as can be concluded on the basis of RMSDs, these effects were quite insignificant. The free energy calculations on optimized conformations of the ion pairs revealed that the free energy of **3a** is 19.6 kJ mol^{-1} lower than that of **3b**. The higher stability of **3a** can be attributed to the presence of an additional weak hydrogen bond formed between N(1) ··· H(1B) and the carboxylic oxygen O(3). The length of this stabilizing hydrogen bond (*i.e.* the N(1) ··· H(1B) distance) is 2.60 Å and the N(1) ··· H(1B) ··· O(3) angle is 139.0°. This result indicates that the association constant for the formation of **3a** is probably higher than that of **3b**.

Experimental

NMR measurements

(*S*)-Mosher acid **2** (Chiraselect, +99% ee), benzene-d_6 (min. 99% D) and chloroform (99.8% D) were purchased from Aldrich. The solutions for determining the variation of $\Delta\delta$ with salt concentration for *rac*-**1** were prepared by diluting a stock solution (139.6 mM) with C_6D_6 to allow final concentrations in the range from 0.1 to 100 mM. Stoichiometric dependence was measured in 30 mM solutions of *rac*-**1**; the acid:base ratio ranged from 0.2 to 3.52. The dependence of the chemical-shift difference ($\Delta\delta$) on enantiomeric composition of **3a** (−90% ee to +95% ee) was determined also for 30 mM solutions in C_6D_6 and in $CDCl_3$ in the presence of 1 equiv. of (*S*)-Mosher acid **2**.

^{1}H and ^{19}F {^{1}H} NMR spectra were recorded on a Bruker AC300 instrument working at 300.13 MHz for ^{1}H and at 282.37 MHz for ^{19}F observation, respectively, using a 5 mm QNP probehead. ^{13}C {^{1}H} NMR spectra were measured at 100.62 MHz on a Bruker AM400. All samples were filtered through a piece of cotton prior to the measurement. Temperature in ^{1}H and ^{19}F {^{1}H} NMR experiments was maintained at 297 or 303 K using a Bruker temperature control unit. Some of ^{13}C {^{1}H} NMR spectra of the diastereomeric mixtures were recorded at 282 K. The samples were spun at 20 Hz. Proton and carbon spectra were calibrated to TMS. Fluorine spectra were referenced externally to $CFCl_3$ (0.0 ppm) in C_6D_6. ^{1}H NMR spectra were collected with a spectral width of 3.6 kHz, size of 32k data points, pulse width of 2 μs (corresponding to the flip angle of 20.9°), repetition delay of 2.0 s, acquisition time of 1.14 s; 16–128 scans were usually accumulated; digital resolution was 0.22 Hz per point. Fluorine and carbon spectra were recorded with proton decoupling. Typical ^{19}F {^{1}H} NMR spectra were obtained with a spectral width of 5.2 kHz, 64k data points, pulse width of 8.6 μs, repetition delay of 2.0 s, acquisition time of 1.59 s; number of scans ranged from 16 to 512, digital resolution was 0.16 Hz per point. ^{13}C {^{1}H} NMR spectra measured on an AM400 were recorded with a spectral width of 29.4 kHz, size of 32k data points, pulse width of 6.7 μs, repetition delay of 2.0 s, acquisition time of 0.46 s; number of scans was usually 1024; digital resolution was 1.84 Hz per point. 2D correlation experiments were carried out using standard pulse programs implemented by the manufacturer. Computer processing of spectra was performed with Bruker WINNMR software. Resolution of 1D spectra was enhanced by applying exponential multiplication or square sine-bell window function (SSB = 2.0) prior to Fourier transformation followed by careful phase and baseline corrections. The corresponding 2D spectra were subjected to resolution enhancement using a square sine-bell windowing and exponential multiplication in F1 direction and in F2 direction, respectively. Complete assignment of all ^{1}H, ^{19}F and ^{13}C resonances in **3a** and **3b** was performed on the basis of a chemical-shift consideration, selective ^{1}H decoupling technique, ^{13}C editing method (DEPT), ^{1}H–^{1}H homonuclear correlations (COSY), ^{13}C–^{1}H heteronuclear correlations (HETCOR, COLOC) and NOE spectroscopy.

X-Ray crystallography

Crystals of **3a** suitable for X-ray diffraction studies were obtained by slow evaporation of a benzene solution. Crystals of **3b** were grown from a cyclohexane–diethyl ether mixture. A single crystal of the salt was mounted in air on a glass fibre. Collection of intensity data was performed at room temperature on an Enraf-Nonius CAD4 single-crystal diffractometer using graphite monochromatized Cu-Kα radiation and θ-2θ scan mode. Unit cell dimensions were determined from the angular setting of 25 reflections. Intensity data were corrected for Lorentz and polarization effects. Semi-empirical absorption correction (ψ-scans)[27] was applied. The structure was solved using the program CRUNCH[28] and was refined anisotropically using full-matrix least full-squares on F^2 (SHELXL97[29]). Crystal data and structure refinement for **3a** and **3b** are given in Table 3. PLUTON drawings[30] of crystal structures are shown in Figs. 5 and 6. For **3a**, all hydrogens, except those attached to N(1) and O(1), were placed at calculated positions and were refined riding on the parent atoms. The hydrogens of the methyl groups were refined as rigid rotors, with idealized sp^3 hybridization and a C–H bond length of 0.97 Å, to match maximum electron density in a difference Fourier map. For **3b**, the hydrogen atoms attached to N(1) and O(1) were taken from a difference Fourier map and were freely refined. Atomic coordinates, bond lengths and angles, and thermal parameters will be deposited at the Cambridge Crystallographic Data Centre (CCDC).†

Conclusion

Diastereomeric salts, **3a** and **b**, formed between enantiomeric bases, **1a** and **b**, and (*S*)-Mosher acid **2**, were investigated by means of NMR spectroscopy and X-ray structural analysis. The chemical shift anisochrony $\Delta\delta$ was detected for some of the nuclei of the piperidinium moiety which were located in close proximity to the complexation site and to the asymmetric centres. In benzene solutions, the magnitude of $\Delta\delta_F$ (for the fluorine nucleus in 4-fluorophenyl group) showed a strong dependence on the concentration, stoichiometric ratio and enantiomeric composition of the diastereomeric salt which suggests that the transient diastereomeric complexes in solution exist in specific conformations and that the association constants for the formation of salt complexes are not equal. This was supported by the results of *ab initio* calculations performed on optimized X-ray conformations of the ion pairs, showing that **3a** is more stable than **3b** which implies that the association constant for its formation may be higher. The X-ray analysis revealed that the solid-state structures of diastereomeric salts, **3a** and **b**, are primarily controlled by hydrogen bonding. The conformations of the piperidinium moiety are essentially identical with respect to interatomic distances, bond and torsion

† CCDC reference numbers 190457 and 190458. See http://www.rsc.org/suppdata/p2/b2/b207176b/ for crystallographic files in .cif or other electronic format.

angles. However, the main structural difference between the ion pairs occurs in the conformations of the (*S*)-Mosher carboxylates and in the mutual configuration of counterions. We suppose that the interactions detected in the solid state also occur in short-lived diastereomeric complexes in solution and that the distinct conformations of the solution complexes, which give rise to the NMR signal anisochrony, resemble those in the solid state.

Acknowledgements

The authors thank Mr Ad Swolfs for his excellent technical assistance in measuring NMR spectra on Bruker AC300. We would also like to thank Synthon BV (The Netherlands) for providing samples of enantiopure **1a** and enantiomerically enriched **1b**. The financial support of the Ministry of Education of the Czech Republic (Grant No. J07/98: 143100011) is gratefully acknowledged.

References

1 D. Parker, *Chem. Rev.*, 1991, **91**, 1441.
2 M. Raban and K. Mislow, *Tetrahedron Lett.*, 1965, 4249.
3 (*a*) W. H. Pirkle, *J. Am. Chem. Soc.*, 1966, **88**, 1837; (*b*) W. H. Pirkle and S. D. Beare, *J. Am. Chem. Soc.*, 1968, **90**, 6250.
4 A. Horeau and J.-P. Guetté, *C. R. Seances Acad. Sci., Ser. C*, 1968, **267**, 257.
5 (*a*) A. Ejchart and J. Jurczak, *Bull. Acad. Pol. Sci.*, 1970, **18**, 445; (*b*) M. Mikolajczyk, A. Mannschreck, V. Jonas and B. Kolb, *Angew. Chem.*, 1973, **85**, 590; (*c*) D. Parker and R. J. Taylor, *Tetrahedron*, 1987, **43**, 5451; (*d*) S. C. Benson, P. Cai, M. Colon, M. A. Haiza, M. Tokles and J. K. Snyder, *J. Org. Chem.*, 1988, **53**, 5335; (*e*) M. J. Shapiro, A. E. Archinal and M. A. Jarema, *J. Org. Chem.*, 1989, **54**, 5826; (*f*) M. A. Haiza, A. Sanyal and J. K. Snyder, *Chirality*, 1997, **9**, 556.
6 R. Fulwood and D. Parker, *J. Chem. Soc., Perkin Trans.2*, 1994, 57.
7 (*a*) C. A. R. Baxter and H. C. Richards, *Tetrahedron Lett.*, 1972, 3357; (*b*) J. D. Roberts and R. Dyllick-Brenzinger, *J. Am. Chem. Soc.*, 1980, **102**, 1166; (*c*) B. E. Maryanoff and D. F. McComsey, *J. Heterocycl. Chem.*, 1985, **22**, 911; (*d*) M. Mikolajczyk, J. Omelanczuk, M. Leitloff, J. Drabowicz, A. Ejchart and J. Jurczak, *J. Am. Chem. Soc.*, 1978, **100**, 7003.
8 F. J. Villani, M. J. Costanzo, R. R. Inners, M. S. Mutter and D. E. McClure, *J. Org. Chem.*, 1986, **51**, 3715.
9 J. A. Dale, D. L. Dull and H. Mosher, *J. Org. Chem.*, 1969, **34**, 2543.
10 (*a*) J. A. Dale, D. L. Dull and H. Mosher, *J. Am. Chem. Soc.*, 1972, **95**, 512; (*b*) S. K. Latypov, J. M. Seco, E. Quinoa and R. Riguera, *J. Am. Chem. Soc.*, 1998, **120**, 877; (*c*) D. R. Kelly, *Tetrahedron: Asymmetry*, 1999, **10**, 2927.
11 (*a*) K. Wypchlo and H. Duddeck, *Chirality*, 1997, **9**, 601; (*b*) S. Hameed, R. Ahmad and H. Duddeck, *Magn. Reson. Chem.*, 1998, **36**, 47; (*c*) S. Malik, H. Duddeck, J. Omelanczuk and M. I. Chounhary, *Chirality*, 2002, **14**, 407.
12 P. Bouř, H. Navrátilová, V. Setnička, M. Urbanová and K. Volka, *J. Org. Chem.*, 2002, **67**, 161.
13 K. L. Dechant and S. P. Clissold, *Drugs*, 1991, **41**, 225.
14 H. Navrátilová, *Magn. Reson. Chem.*, 2001, **39**, 727.
15 W. H. Pirkle and D. J. Hoover, *Top. Stereochem.*, 1982, 264.
16 W. H. Pirkle and T. C. Pochapsky, *J. Am. Chem. Soc.*, 1987, **109**, 5975.
17 (*a*) A. Ejchart and J. Jurczak, *Bull. Acad. Pol. Sci.*, 1971, **19**, 721; (*b*) A. Ejchart and J. Jurczak, *Bull. Acad. Pol. Sci.*, 1971, **19**, 725.
18 S. P. Zingg, E. M. Arnett, A. T. McPhail, A. A. Bothner-By and W. R. Gilkerson, *J. Am. Chem. Soc.*, 1988, **110**, 1565.
19 D. Parker, R. J. Taylor, G. Ferguson and A. Tonge, *Tetrahedron*, 1986, **42**, 622.
20 R. Taylor and O. Kennard, *Acc. Chem. Res.*, 1984, **17**, 320.
21 R. Yoshioka, H. Hiramatsu, K. Okamura, I. Tsujioka and S. Yamada, *J. Chem. Soc., Perkin Trans.2*, 2000, 2121.
22 P. Hobza and Z. Havlas, *Chem.Rev.*, 2000, **100**, 4253.
23 K. B. Lipkowitz, *Acc. Chem. Res.*, 2000, **33**, 555.
24 B. S. Jursic and Z. Zdravkovski, *J. Org. Chem.*, 1993, **58**, 5245.
25 M. J. Frisch, G. W. Trucks, H. B. Schlegel, P. M. W. Gill, B. G. Johnson, M. A. Robb, J. R. Cheeseman, T. Keith, G. A. Petersson, J. A. Montgomery, K. Raghavachari, M. A. Al-Laham, V. G. Zakrzewski, J. V. Ortiz, J. B. Foresman, J. Cioslowski, B. B. Stefanov, A. Nanayakkara, M. Challacombe, C. Y. Peng, P. Y. Ayala, W. Chen, M. W. Wong, J. L. Andres, E. S. Replogle, R. Gomperts, R. L. Martin, D. J. Fox, J. S. Binkley, D. J. Defrees, J. Baker, J. P. Stewart, M. Head-Gordon, C. Gonzales and J. A. Pople, GAUSSIAN 94, Revision D.4, Gaussian, Inc., Pittsburgh, PA, 1995.
26 D. Buttar, M. H. Charlton, R. Docherty and J. Starbuck, *J. Chem. Soc., Perkin Trans.2*, 1998, 763.
27 A. C. T. North, D. C. Philips and F. S. Mathews, *Acta Crystallogr., Sect. A*, 1968, **24**, 351.
28 R. de Gelder, R. A. G. Graaff and H. de Schenk, *Acta Crystallogr., Sect. A*, 1993, **49**, 287.
29 G. M. Sheldrick, SHELXL-97, Program for the Refinement of Crystal Structures, University of Göttingen, Germany, 1997.
30 A. L. Spek, PLUTON, A Program for Plotting Molecular and Crystal Structures, University of Utrecht, The Netherlands, 1995.